International Symposium COMODIA 90: 601-605(1990)

Modelling of Droplet-Gas Interaction in a Spray Combustion Engine

J.N.Chung, T.R.Troutt and C.T.Crowe

Washington State University
P.O. Box 2920
Pullman, WA 99164
U.S.A.

ABSTRACT

The mixing of droplet with carrier gas flow in turbulent free shear layers is important to many natural and industrial processes. Free shear layers are characterized by large scale turbulent structures which evolve and interact with time. These vortical structures usually found in a spray combustor play a major role in droplet mixing and dispersion. The rotational motion of the structures gives rise to a centrifuging effect which displaces the droplet from the vortex cores and enhances dispersion. The degree of dispersion depends on the Stokes number or the ratio of droplet repsonse time to fluid interaction time.

Numerical simulations of droplet dispersion have been developed using the trajectory method in concert with the discrete vortex approach for the carrier phase. The discrete vortex method models the pairing and growth of the large scale structures and provides a velocity field for integration of droplet trajectories. These numerical studies show the centrifuging effect of rotating structures on the droplet dispersion phenomena.

The complementary experimental and numerical results provide an improved understanding of droplet dispersion in large scale turbulent structures found in a spray combustion environment.

INTRODUCTION

The dispersion of droplets in liquid sprays is key element in the design and performance of combustion systems using liquid fuels.

The traditional approach to modeling droplet dispersion in turbulent flow is to treat the phenomena as a Fickian diffusion process in which the diffusional mass flux is jointly proportional to a diffusion coefficient and concentration gradient. Currently the most popular numerical approach for predicting droplet dispersion in turbulence is the Monte-Carlo method in which the turbulent field is represented with a random number generator. This numerical approach and other studies relating to particle dispersion in turbulent flows have been reviewed in a paper by Crowe, Chung and Troutt (1). The majority of applications including the spray combustion involve the mixing of two streams of unequal velocity such as free shear flows.

Mixing layers, jets and wakes are examples of free shear flows that have received considerable attention over the past 15 years as a result of the revolutionary experiments by Brown and Roshko (2) and Winant and Browand (3). These pioneering studies demonstrated that large-scale organized vortex structures were the dominant component of the turbulent shear flows. The pairing of these like signed vortical structures, as they move downstream, is related directly to the lateral growth of the mixing layer.

Over the past five years, a group at Washington State University has carried out extensive numerical and experimental studies on the influence of large scale vortex structures in free shear flows. These efforts were initiated in an attempt to validate a concept for particle dispersion first proposed by Crowe et al. (4). They postulated that particle dispersion depends strongly on the Stokes number, $\gamma_\tau = \tau_A/\tau_F$, which is the ratio of particle aerodynamic response time to the characteristic time of the flow field. The time scale associated with the flow field is

$$\tau_F = \delta/\Delta U \tag{1}$$

where δ is the size of the structure and ΔU is the velocity difference across the mixing layer. The aerodynamic response time,

$$\tau_A = \rho_p d^2/18\mu, \tag{3}$$

A pictorial representation of the importance of Stokes number is shown in Fig. 1. For small values of the Stokes numbers, the droplets have sufficient time to respond to the fluid motion and will disperse as fluid droplets. For large values the droplets will have insufficient time to respond to the large scale structures and will move in nearly linear trajectories. For intermediate values the particles become entrained in the vortices and are centrifuged away from the vortex cores giving rise to a dispersion rate which exceeds that of a fluid particle.

NUMERICAL METHODS

Following the numerical simulation efforts of Chung and Troutt (5) and Chein and Chung (6) a two-dimen sional, inviscid discrete vortex numerical technique was developed to simulate the mixing layer flow. The particle

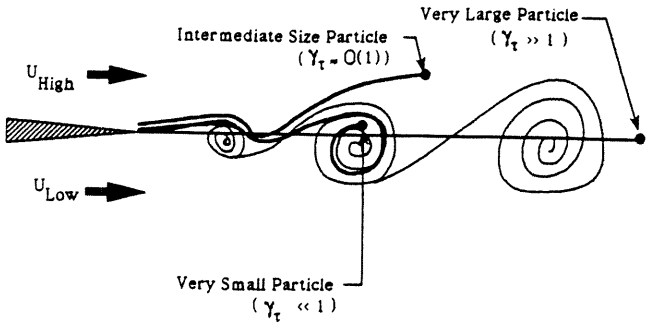

FIG. 1. Hypothesized model for particle dispersion in a plane mixing layer.

motion was then computed using a modified Stokes force relationship(Crowe, Gore and Troutt (4)). Details concerning the numerical procedures can be found in Refs. 5 and 6. The simulation results employed here in addition used a conformal mapping technique such that the effects of the bounding tunnel walls could also be included in the model through a zero normal velocity condition following Ghoniem and Ng (7). The numerical effort was also aimed at simulating the test facility geometry and experimental conditions as closely as possible under the limitations of the basic assumptions in the discrete vortex model.

RESULTS AND DISCUSSION

Fig. 2a shows typical instantaneous discrete vortex patterns from the numerical simulation for nonforced mixing layer. The associated instantaneous vorticity contours are shown in Fig. 2b. Large scale vortex structures, represented by the clusters of discrete vortex elements are evident in the figures. Pairing interaction, as can be seen in the middle of the figures, starts with the upstream vortex moving slightly up into the high-speed stream and acquires a faster speed. It catches up the preceding one from above, coalesces and forms a new identity. Between two large scale structures, the vorticity is stretched and braids are formed. This braid region is found to play an important role in the particle dispersion process. It is the bridge through which particles of γ_τ's of O(1) are dispersed across the mixing layer. Fig. 2c clearly illustrates the formed particle sheets between the large scale structures.

The numerical results can also be evaluated from a quantitative time average sense. Fig. 3 shows time average downstream mean velocity profiles. The profiles are non-dimensionalized by local flow properties and compared to a curve fit involving the tanh function and its derivative previously employed by Gaster, Kit and Wygnanski (8), for fitting mixing layer experimental data. This functional form provided a better fit for the experimental data than the conventional simple tanh profile used previously by numerous investigators.

Root mean square velocity fluctuation levels for downstream and cross-stream velocity components are shown in Figs. 4a and b. The maximum intensity of the downstream fluctuation u', when non-dimensionalized by the velocity difference (i.e. $u'/\Delta U = 0.18$), is somewhat

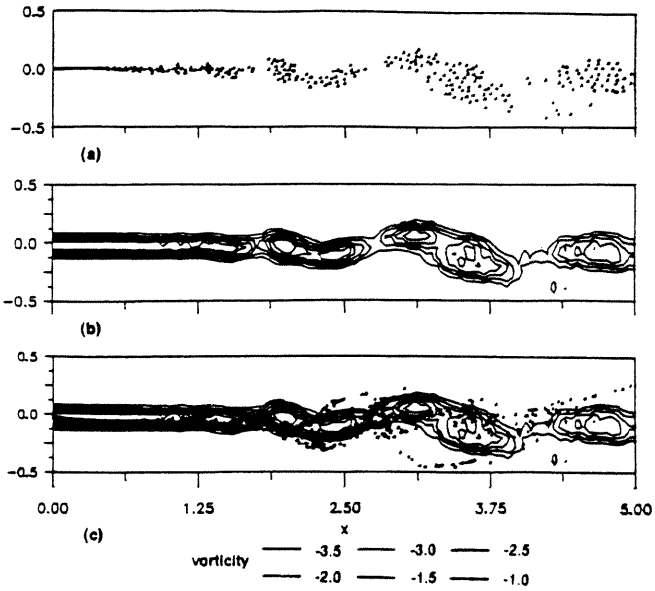

FIG. 2. Instantaneous vortex and particle patterns: (a) vortex patterns, (b) vorticity contours, and (c) vorticity contours and particle streaklines.

higher than the measured value 0.13 in our mixing layer flow using hot-wire and Browand and Latigo's value 0.15 (Ref. to 9). However, it is in good agreement with Oster and Wygnanski's results (10) (also 0.18). Furthermore, the total non-dimensionalized fluctuation energy $(u'^2 + v'^2)/2\Delta U^2$ for the current two dimensional numerical simulation gives 3.83 x 10^{-2}, it compares favorable to the total fluctuation energy measurements $(u'^2 + v'^2 + w'^2)/2\Delta U^2$ in the three dimensional mixing layer (10) (3.84 x 10^{-2}), indicating that the spamwise fluctuation w' is redistributed between two dimensions in the simulations.

Particles of monosize distribution are released uniformly from cross-stream positions at x=0. To evaluate the Stokes number γ_τ, the large scale structure characteristic time is chosen as the reciprocal of the natural initial instability frequency, calculated from the velocity component near the mixing layer origin. Fig. 5 shows the instantaneous patterns for tracers and particles with γ_τ's of the order of 0.1, 1 and 10 (from top to bottom). Similar to smoke visualizations, tracers once get entrained into the mixing layer are trapped in the vortex cores. Larger particles with γ_τ's of O(0.1) start to move towards edges of the large scale structures. Particles with γ_τ's of O(1) are clearly thrown out of the vortical structures, and yield the largest dispersion. Further increase in the γ_τ results in a sharp decrease in the dispersion, as shown in the case of γ_τ's of O(10). The particle dispersion patterns from the numerical simulations are qualitatively in good agreement with the visualization pictures and indicate that the Stokes number γ_τ is indeed the parameter to describe the particle dispersion in the large scale structures, as proposed by Crowe, Gore and Troutt (4).

Time average particle concentration profiles with γ_τ's of O(1) were also obtained from the numerical simulations by releasing numerous particles in the neighborhood of the mixing layer origin x = 0, y = 0. The results of these simulated concentration profiles are shown in

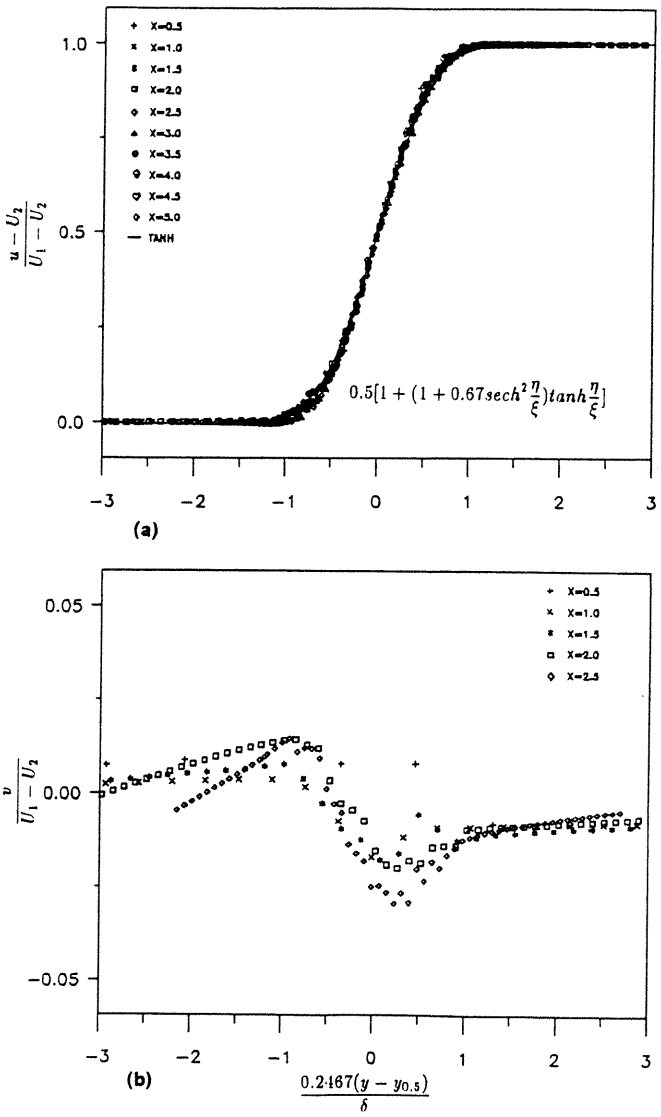

FIG. 3. Time average downstream mean velocity profiles from numerical simulations: (a) downstream component, (b) cross-stream component.

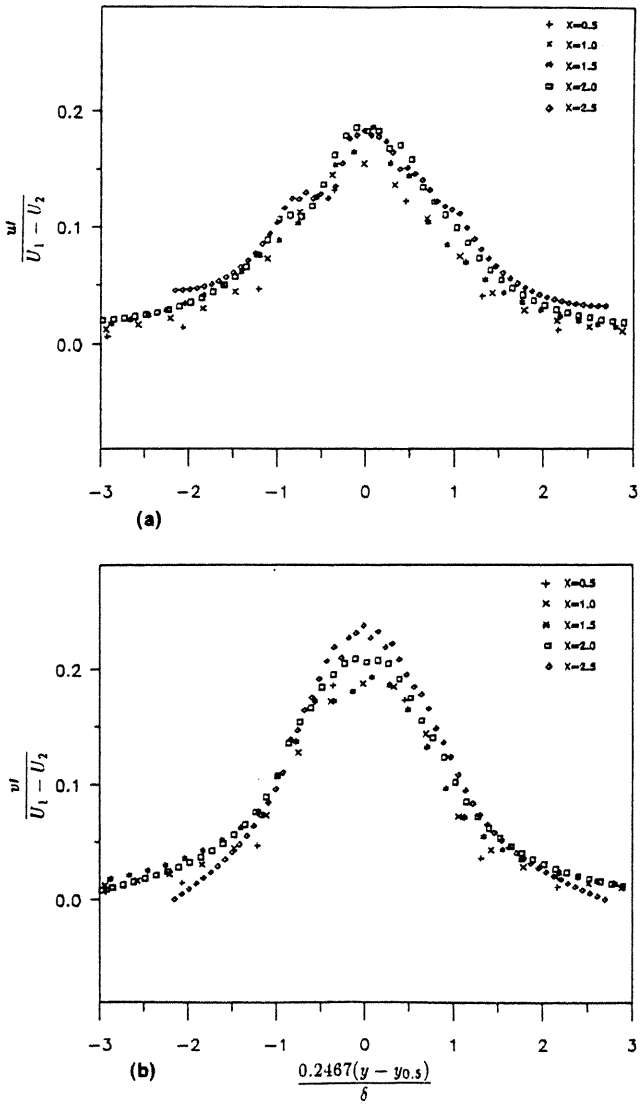

FIG. 4. RMS velocity fluctuation levels from numerical simulations: (a) downstream component, and (b) cross-stream component.

Fig. 6. The simulated profiles show much of the same character as the experimental profiles, developing a double peak nature at early downstream positions followed by the movement of a single peak gradually below the centerline.

To more closely examine the mixing mechanism of the solid particles the instantaneous vorticity contours and particle patterns are shown in Fig. 7. Detailed observation of the particle patterns appear to indicate that the mixing mechanism can be divided into two parts. One part appears to be a stretching mechanism associated with the high velocity gradient braid regions connecting the high and low speed boundaries of adjacent vortex structures. The rotational nature of the large vortex structures tends to rapidly separate neighboring particles in these regions. This mechanism tends to produce and stretch sheets of particles which ride on the back side of the upstream large scale vortices or are flung centrifugally into the high speed stream (Fig. 7a). The second mechanism appears to be associated with the pairing interactions of adjacent large scale vortices. These pairing interactions tend to fold the particle sheets down onto themselves towards the low speed side of the mixing layer (in the middle of Fig. 7b). In addition, a schematic illustrating these concepts is shown in Fig. 8.

One important point concerning the stretching and folding mechanism described here is that it is qualitatively identical to the stretching and folding mechanism associated with chaotic dynamic systems occurring in phase space. Ottino (11) has recently pointed out that mixing in turbulent flows may be the clearest connection between chaotic dynamics and turbulent flow processes.

ACKNOWLEDGMENT

The authors gratefully acknowledge the support of this research by the Department of Energy under grant No. FG06-86ER1333567.

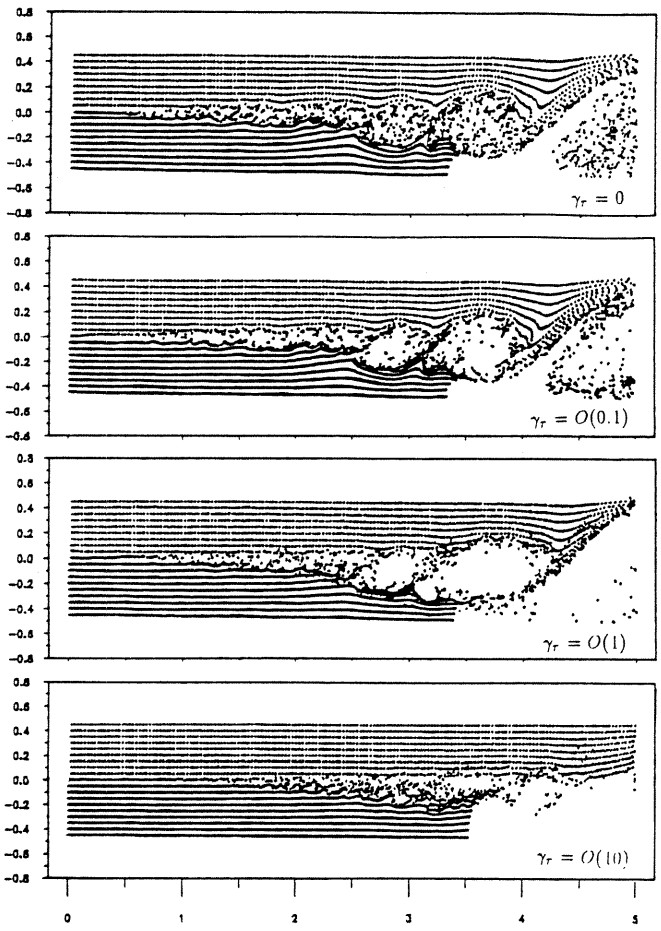

FIG. 5. Instantaneous particle dispersion patterns for tracers and particles with γ_T of O (0.1), O(1) and O(10) (from top to bottom).

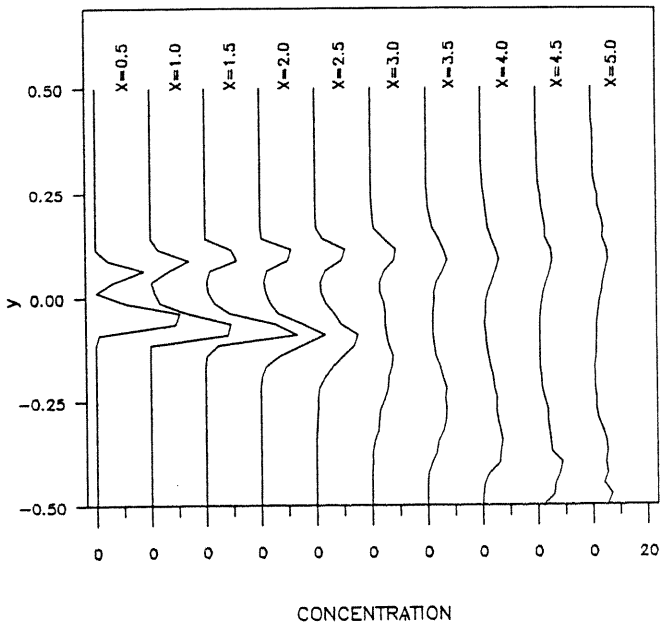

FIG. 6. Profiles of time average particle concentration from numerical simulations.

REFERENCES

1. Crowe, C.T., Chung J.N. and Troutt, T.R., Progress in Energy and Combustion Sci., 14, 171 (1988).
2. Brown, G. and Roshko, A., J. Fluid Mech., 64, 775(1974).
3. Winant, D. and Browand, F.K., J. Fluid Mech., 63, 237(1974).
4. Crowe, C.T., Gore, R.A. and Troutt, T.R., Particulate Science and Tech. J., 3, 149(1985).
5. Chung, J.N. and Troutt, T.R., J. Fluid Mech., 86, 199(1988).
6. Chein, R. and Chung, J.N., AlChE J, 34. (6), 946(1988).
7. Ghoniem, A.F. and Ng, K.K., Phys. Fluid, 30, (3) 706(1987).
8. Gaster, M., Kit, E. and Wygnanski,I., J. Fluid Mech., 150, 23(1985).
9. Browand, F.K. and Latigo, B.O., Phys. Fluids, 22, 1011(1979).
10. Oster, D. and Wygnanski, I., J. Fluid Mech., 123, 91(1982).
11. Ottino, J.M., Ann. Rev. Fluid Mech., 22, 207 (1990).

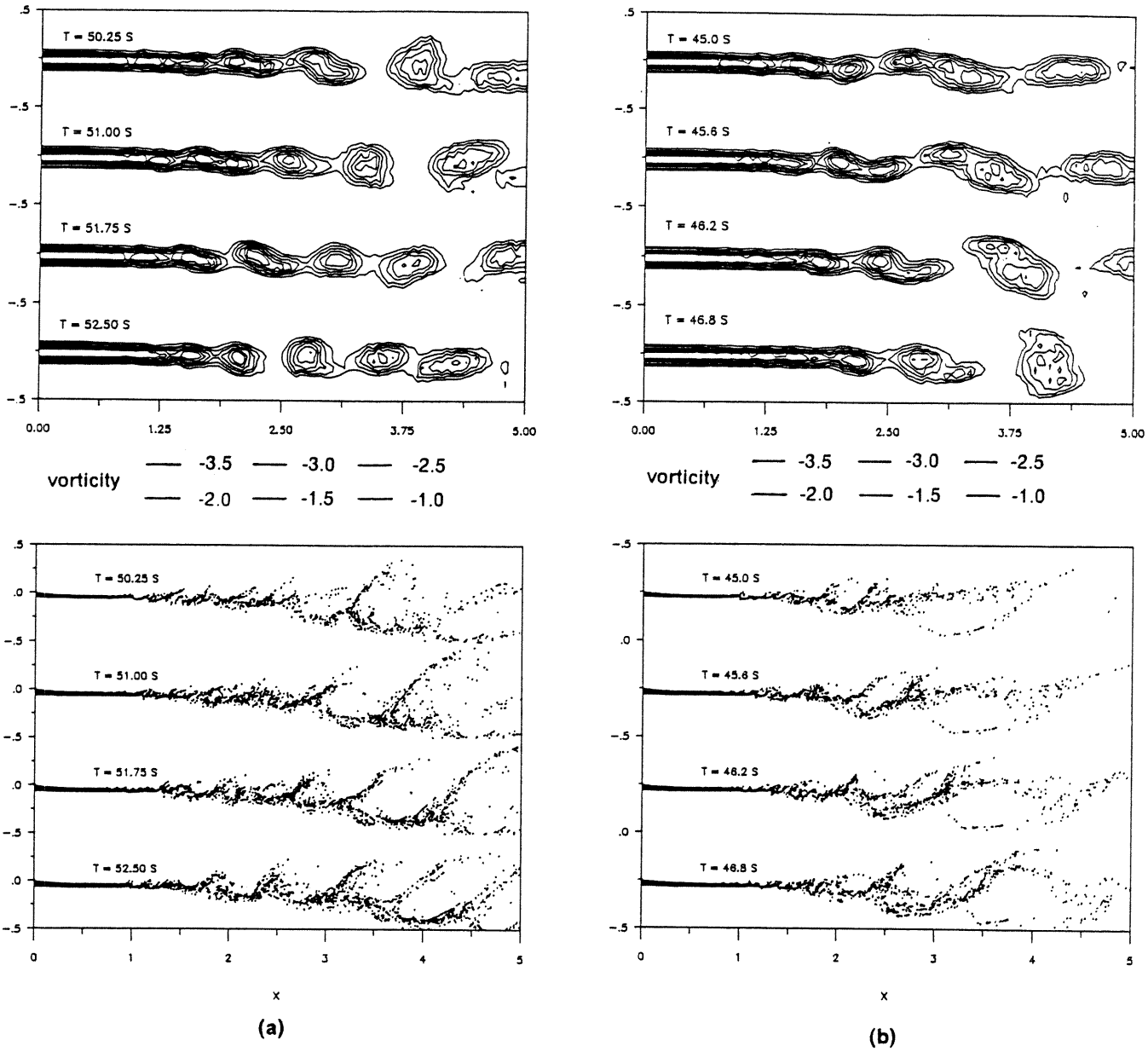

FIG. 7. Instantaneous vorticity contours and particle streaklines with γ_T's of O(1) at successive times: (a) stretching, and (b) folding.

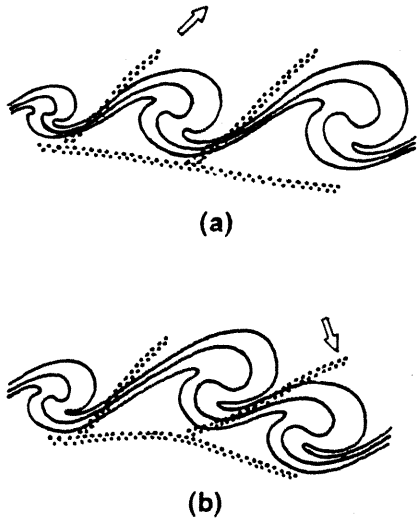

FIG. 8. Schematic illustrating particle dispersion mechanism: (a) stretching of particle streaklines, and (b) folding of particle streaklines.